J. Mech. Phys. Solids Vol. 27, pp. 465–487
© Pergamon Press Ltd. 1979. Printed in Great Britain

0022-5096/79/1201-0465 $02.00/0

A CLASS OF PHENOMENOLOGICAL CORNER THEORIES OF PLASTICITY

J. CHRISTOFFERSEN

Department of Solid Mechanics,
Technical University of Denmark, DK-2800 Lyngby, Denmark

and

J. W. HUTCHINSON

Division of Applied Sciences,
Harvard University, Cambridge, MA 02138, U.S.A.

(*Received* 6 *February* 1979)

ABSTRACT

A CLASS of phenomenological flow theories of plasticity is proposed which models time-independent incremental behavior at a corner of the yield surface of a polycrystalline metal. The proposal is consistent with the physical theories of plasticity based on single crystal slip. Conditions for convexity, ensuring invertibility of the incremental relations, are derived. The simplest candidate, called J_2 corner theory, coincides with the J_2 deformation theory of plasticity for nearly proportional stress increments and incorporates a smooth transition to elastic unloading for increasingly non-proportional increments. The theory is applied to the bifurcation and imperfection-sensitivity analysis of necking in a thin sheet. For this example, like many others involving bifurcation in the plastic range, the corner theory appears to circumvent some of the difficulties associated with use of the standard phenomenological plasticity laws.

1. INTRODUCTION

TO MOTIVATE the introduction of a corner theory of plasticity, we begin by reviewing the unsatisfactory state of affairs which has existed for some years with respect to bifurcation-related phenomena in the plastic range, such as buckling and necking.

Since the late 1940's evidence has been accumulating related to the inadequacy of buckling predictions from bifurcation analyses using the classical flow theory of plasticity with a smooth yield surface. Whenever buckling involves an abrupt change in the relative proportions of the components of the stress increments, the bifurcation load or deformation from any of the classical flow theories overestimates findings from buckling experiments, in some instances by a considerable amount. Bifurcation predictions based on deformation theories of plasticity are generally in much better agreement with tests. In engineering applications it is almost always formulas based on J_2 deformation theory which are used to estimate buckling loads or deformations, with due recognition of the effect of initial imperfections especially in the case of shell-type structures.

Studies of some simple examples, such as the cruciform column under axial compression, indicate that accounting for very small initial imperfections reduces the discrepancies between the two theories. Imperfections, so small that they must be considered to be unavoidable, reduce the flow theory buckling load to a level which is close to the bifurcation load of deformation theory. Tests on cruciform columns reveal relatively little scatter and are consistently in accord with the bifurcation results from deformation theory. It follows, then, that use of a flow theory with a smooth yield surface seems to result in an unobservable material-based sensitivity to extremely small imperfections which renders the bifurcation load from this theory to be of essentially no significance.

The situation with respect to necking in thin metal sheets subject to biaxial tensile stretching has been less thoroughly explored but recent work suggests a close parallel to that for buckling just described, except for one important point. Calculations based on a flow theory with a smooth yield surface give necking-type bifurcations at strain levels which far exceed realistic values, while bifurcation strains from deformation theory are at least in qualitative agreement with observation. Inclusion of realistic levels of initial imperfections does not appear to reduce the classical flow theory results by a sufficient amount to produce agreement with test data. Necking takes place much deeper into the plastic range than is generally the case in buckling, and this may be why unavoidably small imperfections reduce the discrepancy between the predictions based on flow and deformation theories in one case and not in the other.

Use of instantaneous moduli from deformation theory in bifurcation calculations was first justified by BATDORF (1949) and later by SANDERS (1954) by appealing to a flow theory with a corner at the loading-point on the yield surface. For nearly proportional loading increments there exists such a flow theory whose instantaneous moduli coincide with those of the corresponding deformation theory. Furthermore, arguments similar to those of SHANLEY (1947), as later generalized by HILL (1961), provide the theoretical rationale for bifurcation taking place under conditions meeting the requirement of nearly proportional loading.

The use of deformation theory is limited to the bifurcation problem. A post-bifurcation response almost always involves strongly non-proportional loading, as does the fully nonlinear response of an initially imperfect realization of the structure near the critical point. Of course, one of the more sophisticated flow theories which permit corner formation, such as the slip theory of BATDORF and BUDIANSKY (1949), could in principle be used to explore both bifurcation and post-bifurcation behavior as well as imperfection-sensitivity. However, slip theory, which is the simplest of the physical theories, is already too complicated to serve as a constitutive law in calculations of this sort, even when computers are employed.

SEWELL (1974) used the theory of multiple yield systems, introduced by KOITER (1953), MANDEL (1965) and HILL (1966), as the basis for constructing a representation at the corner of a yield surface. He restricted consideration to base states of uniaxial stress. For total loading increments from the base state in which all yield systems are active, Sewell was able to choose the parameters characterizing the systems such that their combined incremental behavior coincides with J_2 deformation theory. With this choice, bifurcation from a state of uniaxial stress would necessarily coincide with the predictions of J_2 deformation theory. As the theory stands, it cannot be used in post-

bifurcation calculations since it is restricted to uniaxial base states. Furthermore, a computationally practical extension of Sewell's representation to general stress states is not obvious.

The purpose of this paper is to present a relatively simple phenomenological corner theory of plasticity suitable for use in numerical calculations of the type described above. The proposal embodies the essential features shared by the physical theories for time-independent plastic deformation of polycrystalline metals based on single crystal slip. Physical theories all imply the formation of a corner at the loading-point on the yield surface. On the other hand, the most recent survey of yield surface experimentation (HECKER, 1976) suggests that, while a surface with relatively high curvature at the loading-point is often observed, sharp corners are seldom seen. With the issue of corners aside, it is generally agreed that the simplest flow theory built upon the assumption of isotropic hardening using the Mises yield surface underestimates certain crucial plastic strain components in a non-proportional stress history such as those encountered in buckling or necking. It is no surprise, therefore, that as a plasticity model it leads to unconservative estimates in buckling or necking applications. A kinematic hardening description of the yield surface will sometimes give a better representation of the local curvature at the loading-point. Its use in sheet necking calculations does lead to more sensible predictions at realistic imperfection levels (TVERGAARD, 1978), even though the bifurcation strains for the perfect sheet are the same unrealistic values as from isotropic hardening.

In contrast to a smooth yield surface characterization, a corner theory will most likely overestimate certain components of the plastic strain increments in the vicinity of an abrupt change from proportional loading. The error in buckling and necking applications will tend to be conservative, although experience with necking and buckling, particularly, suggests this error may not be very large.

Thus, without taking a position on the debate eternal on the experimental existence of corners, we propose the following corner theory as an alternative to the standard theories in the spirit described above. As has already been mentioned, the bifurcation point retains a significant role in the analysis of buckling or necking when a corner theory is used, which is not the case when a smooth yield surface description is employed. This virtue of corner theory should not be discarded lightly.

The general phenomenological corner theory presented in Section 2 differs somewhat from an earlier version of CHRISTOFFERSEN (1978), which is discussed in relation to the present version in the Appendix. The simplest corner theory, J_2 corner theory, is given in Section 3. To illustrate use of the theory it is applied to the analysis of necking in a thin sheet under biaxial stretching. The corner theory yields the bifurcation results of STÖREN and RICE (1975) together with an assessment of post-bifurcation behavior and imperfection-sensitivity.

For the most part a standard compact tensor notation is employed. Bold-face lower case letters designate symmetric second-order tensors. In this paper, all fourth-order tensors share the following indicial symmetries in their Cartesian components:

$$A_{ijkl} = A_{jikl} = A_{ijlk} = A_{klij};$$

they are represented by upper case bold-face letters. The following standard notation for contracted products is used: **Aa** ($A_{ijkl}a_{kl}$ in Cartesian components); **ab** ($a_{ij}b_{ij}$); and

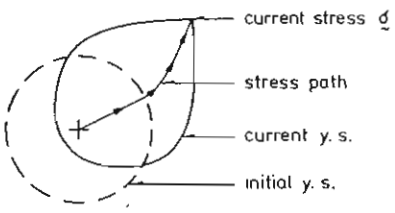

FIG. 1. Typical stress history in a bifurcation-related problem.

Aab = **Aba** ($A_{ijkl}a_{ij}b_{kl}$). The tensor product with Cartesian components $a_{ij}a_{kl}$ is denoted by $\mathbf{a} \otimes \mathbf{a}$. If desired, the notation can be converted to a matrix–vector representation.

2. INCREMENTAL RELATIONS FOR CORNER THEORY

2.1 *Preliminaries*

As discussed in the Introduction, we are primarily concerned with stress histories, such as that depicted in Fig. 1, which involve continuing plastic deformation on paths which may undergo abrupt changes in direction, and even elastic unloading, but not reversed plastic flow. The corner forms at the loading-point as the virgin yield surface is penetrated, and it is pushed along by the loading-point until elastic unloading occurs. HILL (1967) has given a general treatment of the essential structure to be expected of time-independent elastic–plastic constitutive laws for polycrystalline metals assuming the mechanism of single crystal slip at the microscopic level. The properties invoked below are shared by all the physical theories, including slip theory and the more elaborate self-consistent models of polycrystals.

Denote the strain-rate by $\dot{\varepsilon}$ and the stress-rate by $\dot{\sigma}$. For the moment we will concentrate on "small strain" plasticity, but at a later stage in the discussion of an extension into the finite strain range, $\dot{\sigma}$ will be identified with the Jaumann rigid-body rate of the Cauchy stress. The instantaneous elastic compliances are assumed to be positive definite and are denoted by $\mathscr{M}$. The elastic and plastic parts of the strain-rate are defined in the usual way as

$$\dot{\varepsilon}^e = \mathscr{M}\dot{\sigma} \quad \text{and} \quad \dot{\varepsilon}^p = \dot{\varepsilon} - \dot{\varepsilon}^e. \tag{2.1}$$

Below, the potential for the strain-rate will be introduced; the elastic part is

$$W^e = \tfrac{1}{2}\mathscr{M}\dot{\sigma}\dot{\sigma}. \tag{2.2}$$

At the microscopic level the material is assumed to strain-harden and to be characterized by standard slip relations (see MANDEL (1965) or HILL (1966)). Minimal restrictions ensure that these relations admit a convex potential function for the plastic strain-rate which is homogeneous of degree two in the stress-rate. From this starting point it can be shown (HILL, 1967) that there exists a convex potential

function of the macroscopic stress-rate, W^p, which is also homogeneous of degree two, such that the macroscopic plastic strain-rate is given by

$$\varepsilon^p = \partial W^p / \partial \dot{\sigma}. \tag{2.3}$$

If $\dot{\sigma}_1$ and $\dot{\sigma}_2$ are any two different stress-rates with associated plastic strain-rates ε_1^p and ε_2^p from (2.3), then convexity requires

$$W^p(\dot{\sigma}_2) - W^p(\dot{\sigma}_1) - (\dot{\sigma}_2 - \dot{\sigma}_1)\varepsilon_1^p \geqslant 0 \tag{2.4}$$

for all such pairs. The function W^p is assumed to be independent of a superimposed hydrostatic pressure-rate and consequently ε^p is volume-preserving. The equality in (2.4) holds if and only if both plastic strain-rates vanish, assuming the deviatoric parts of the stress-rates to differ. Convexity guarantees the invertibility of the relation between the strain-rate and stress-rate given below.

Drucker's postulated condition for a stable material is contained in (2.4) and is retrieved immediately by taking $\dot{\sigma}_2 = 0$ and using $W^p(\dot{\sigma}_1) = \frac{1}{2}\dot{\sigma}_1 \varepsilon_1^p$, i.e.

$$\dot{\sigma}\varepsilon^p \geqslant 0. \tag{2.5}$$

Other known conditions holding at a corner which follow from (2.4) will be seen below. The total potential, $W = W^e + W^p$, is strictly convex and provides the total strain-rate as

$$\varepsilon = \partial W / \partial \dot{\sigma}. \tag{2.6}$$

2.2 *The plastic potential* $W^p(\dot{\sigma})$

The corner of the yield surface will be specified by taking the boundary of the elastic unloading region to be a generalized cone in deviatoric stress-rate space as depicted in Fig. 2(a). Let λ be the symmetric deviator tensor directed along the axis of this cone and let θ, to be defined precisely below, be the inherently positive measure of the direction of the stress-rate from the cone axis. The conical surface separating elastic unloading and plastic flow is taken as $\theta = \theta_c$.

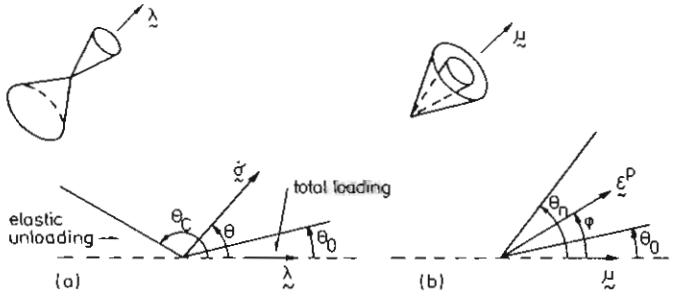

FIG. 2. (a) Stress-rate space; (b) strain-rate space.

For stress-rates falling within the range $\theta \leqslant \theta_0$, the relation between the stress-rate and plastic strain-rate is linear and is written as

$$\boldsymbol{\varepsilon}^{\mathrm{p}} = \mathbf{C}\dot{\boldsymbol{\sigma}}. \tag{2.7}$$

This is the *total loading range* in the terminology of SANDERS (1954) and BUDIANSKY (1959), while HILL (1967) calls it the *fully active range*. It corresponds to that range of $\dot{\boldsymbol{\sigma}}$ for which all *potentially active* slip systems in the polycrystal *remain active*. For $\theta_0 < \theta < \theta_c$, the relation between the plastic strain-rate and stress-rate is nonlinear, although homogeneous of degree one, in a way which must provide a continuous transition from (2.7) to $\boldsymbol{\varepsilon}^{\mathrm{p}} = 0$ for $\theta \geqslant \theta_c$. The possibility of thoroughly nonlinear behavior, in Hill's terminology, with no linear range (i.e. $\theta_0 = 0$) will also be considered as a limiting case. The plastic strain-rate always falls within the forward cone of normals, as elaborated on below; and it will be seen that θ_0 cannot be chosen in excess of $\theta_c - \frac{1}{2}\pi$.

The plastic total loading compliances $\mathbf{C}$ possess the indicial symmetries noted in the Introduction. In addition, if $\boldsymbol{\varepsilon}^{\mathrm{p}}$ is to be deviatoric with no dependence on the deviatoric part of $\dot{\boldsymbol{\sigma}}$, it is required that (in Cartesian components)

$$C_{kkij}(=C_{ijkk}) = 0. \tag{2.8}$$

The plastic total loading compliances are required to be positive definite in the restricted sense that $\mathbf{Caa} > 0$ for all symmetric tensors $\mathbf{a}$ with nonzero deviatoric part. Of course, $\mathbf{C}$ and $\boldsymbol{\lambda}$ will depend on the current state of stress and possibly on the entire stress history. In the simplest specialization of the theory given in Section 3, $\boldsymbol{\lambda}$ will be taken to be proportional to the stress deviator and $\mathbf{C}$ will be identified with the instantaneous "plastic" compliances from J_2 deformation theory.

In the total loading range, $W^{\mathrm{p}} = \frac{1}{2}\mathbf{C}\dot{\boldsymbol{\sigma}}\dot{\boldsymbol{\sigma}}$. To bridge the gap between total loading and elastic unloading we take

$$W^{\mathrm{p}}(\dot{\boldsymbol{\sigma}}) = \tfrac{1}{2} f(\theta)\mathbf{C}\dot{\boldsymbol{\sigma}}\dot{\boldsymbol{\sigma}}, \tag{2.9}$$

where

$$f(\theta) = \begin{cases} 1, & \theta \leqslant \theta_0, \\ 0, & \theta \geqslant \theta_c. \end{cases} \tag{2.10}$$

In the transition range, $\theta_0 \leqslant \theta \leqslant \theta_c$, f will be chosen such that the convexity condition (2.4) is satisfied and such that $\boldsymbol{\varepsilon}^{\mathrm{p}}$ varies continuously with $\dot{\boldsymbol{\sigma}}$ at $\theta = \theta_0$ and at $\theta = \theta_c$.

It will be convenient to introduce the deviatoric tensor

$$\boldsymbol{\mu} = \mathbf{C}\boldsymbol{\lambda} \tag{2.11}$$

and to normalize $\boldsymbol{\lambda}$ such that

$$\mathbf{C}\boldsymbol{\lambda}\boldsymbol{\lambda} = 1 \quad \text{or} \quad \boldsymbol{\mu}\boldsymbol{\lambda} = 1.\dagger \tag{2.12}$$

The direction of the stress-rate measured from the cone axis is defined to be

$$\cos\theta = \frac{\mathbf{C}\boldsymbol{\lambda}\dot{\boldsymbol{\sigma}}}{(\mathbf{C}\dot{\boldsymbol{\sigma}}\dot{\boldsymbol{\sigma}})^{\frac{1}{2}}} = \frac{\boldsymbol{\mu}\dot{\boldsymbol{\sigma}}}{(\mathbf{C}\dot{\boldsymbol{\sigma}}\dot{\boldsymbol{\sigma}})^{\frac{1}{2}}}. \tag{2.13}$$

† Without this normalization, $\boldsymbol{\lambda}$ and $\boldsymbol{\mu}$ need only be replaced by $\boldsymbol{\lambda}/(\boldsymbol{\mu}\boldsymbol{\lambda})$ and $\boldsymbol{\mu}/(\boldsymbol{\mu}\boldsymbol{\lambda})$, respectively, in the subsequent formulas.

Other definitions of θ are possible and might appear simpler. However, the choice (2.13), in which $\mathbf{C}$ plays the role of a metric, leads to an exceptionally attractive interpretation of the convexity condition, as was noted in the different formulation of CHRISTOFFERSEN (1978) discussed in Section 3 and in the Appendix. The definition (2.13), together with $\theta = \theta_c$, specifies the local form of the corner in stress space. The link-up between the yield surface in stress space and the cone in stress-rate space will be made for a special case in Section 3. From (2.13), θ is obviously homogeneous of degree zero in $\dot{\boldsymbol{\sigma}}$ so that W^p in (2.9) is homogeneous of degree two in $\dot{\boldsymbol{\sigma}}$, as required. Since $2W^p = \dot{\boldsymbol{\sigma}}\boldsymbol{\varepsilon}^p$, (2.5) requires f to be non-negative.

The plastic strain-rate can be determined using (2.3) with the result

$$\boldsymbol{\varepsilon}^p = f(\theta)[(1 - k(\theta)\cot\theta)\mathbf{C} + k(\theta)(\sin\theta\cos\theta)^{-1}\boldsymbol{\mu}\otimes\boldsymbol{\mu}]\dot{\boldsymbol{\sigma}}, \tag{2.14}$$

where

$$k(\theta) = -\tfrac{1}{2}f'/f \equiv [\ln(1/f^1)]' \tag{2.15}$$

and where the prime denotes differentiation with respect to the function argument. For $\dot{\boldsymbol{\sigma}}$ co-directional to $\boldsymbol{\lambda}$ so that $\theta = 0$, (2.14) gives $\boldsymbol{\varepsilon}^p$ co-directional with $\boldsymbol{\mu}$. Thus, $\boldsymbol{\mu}$ is directed along the corresponding cone axis in plastic strain-rate space. This statement also holds true for thoroughly nonlinear behavior if $f(0) = 1$ and $f' = f'' = 0$ at $\theta = 0$.

2.3 *Convexity and the transition function* $f(\theta)$

It will now be shown that the convexity condition (2.4) can be reduced to an equivalent condition for the convexity of a certain planar curve specified by $f(\theta)$, together with one side condition.

Since W^p is homogeneous of degree two in the deviatoric stress-rate, it is easy to show that the investigation of convexity can be restricted to the consideration of all deviatoric stress-rates satisfying

$$W^p(\dot{\boldsymbol{\sigma}}) = \tfrac{1}{2}. \tag{2.16}$$

Any deviatoric stress-rate can be written as $\dot{\boldsymbol{\sigma}} = a\boldsymbol{\lambda} + b\boldsymbol{\chi}$ where $\boldsymbol{\chi}$ is a "unit" deviatoric tensor orthogonal to $\boldsymbol{\lambda}$, *viz.*

$$\mathbf{C}\boldsymbol{\chi}\boldsymbol{\chi} = 1 \quad \text{and} \quad \mathbf{C}\boldsymbol{\lambda}\boldsymbol{\chi} = 0. \tag{2.17}$$

The definition (2.13), together with (2.16) and (2.9), implies that any such stress-rate is

$$\dot{\boldsymbol{\sigma}} = (\cos\theta\,\boldsymbol{\lambda} + \sin\theta\,\boldsymbol{\chi})/f^1(\theta). \tag{2.18}$$

Let $\dot{\boldsymbol{\sigma}}^*$ be any other deviatoric stress-rate satisfying (2.16); $\boldsymbol{\chi}^*$ can be found satisfying (2.17) such that

$$\dot{\boldsymbol{\sigma}}^* = (\cos\theta^*\,\boldsymbol{\lambda} + \sin\theta^*\,\boldsymbol{\chi}^*)/f^1(\theta^*). \tag{2.19}$$

Using $2W^p = \dot{\boldsymbol{\sigma}}\boldsymbol{\varepsilon}^p = 1$ in (2.4) (with $\dot{\boldsymbol{\sigma}}_1 = \dot{\boldsymbol{\sigma}}$, $\dot{\boldsymbol{\sigma}}_2 = \dot{\boldsymbol{\sigma}}^*$ and $\boldsymbol{\varepsilon}^p_1 = \boldsymbol{\varepsilon}^p$), the convexity condition becomes

$$1 - \dot{\boldsymbol{\sigma}}^*\boldsymbol{\varepsilon}^p \geqslant 0. \tag{2.20}$$

Next, $\dot{\sigma}^*\varepsilon^p$ is evaluated using the representations (2.18) and (2.19) together with (2.14). With the use of standard trigonometric identities one can arrange the inequality (2.20) into the following form:

$$1-\dot{\sigma}^*\varepsilon^p = 1-(f/f^*)^{\frac{1}{2}}[\cos(\theta^*-\theta)-k\sin(\theta^*-\theta)] + (f/f^*)^{\frac{1}{2}}(1-k\cot\theta)\sin\theta\sin\theta^*(1-C\chi\chi^*)\geqslant 0, \quad (2.21)$$

where $f=f(\theta)$, $f^*=f(\theta^*)$ and $k=k(\theta)$.

For any $\dot{\sigma}^*$ and $\dot{\sigma}$ such that $\theta^*=\theta$ with $\chi^*\neq\chi$, (2.21) requires that

$$1-k(\theta)\cot\theta\geqslant 0 \quad (2.22)$$

since $C\chi\chi^*<1$ if $\chi\neq\chi^*$. Next consider stress-rate pairs such that $\chi^*=\chi$ but $\theta^*\neq\theta$. Then, (2.21) becomes

$$1-(f/f^*)^{\frac{1}{2}}[\cos(\theta^*-\theta)-k\sin(\theta^*-\theta)]\geqslant 0, \quad (2.23)$$

Conversely, if (2.22) and (2.23) are satisfied for all θ and θ^*, then (2.21) is always satisfied. Equations (2.22) and (2.23) are necessary and sufficient conditions for convexity of W^p.

Condition (2.22) is easily met in choosing $f(\theta)$; its implications will be seen later. The second condition (2.23) is the convexity condition for the following planar curve. Let $\mathbf{i}$ and $\mathbf{j}$ be orthogonal unit vectors in the two-dimensional plane, and let θ be measured from $\mathbf{i}$ as shown in Fig. 3(a). Define a curve $\mathbf{v}(\theta)$, where $\mathbf{v}$ is a vector from the origin to the curve, according to

$$\mathbf{v}(\theta)=(\cos\theta\,\mathbf{i}+\sin\theta\,\mathbf{j})/f^{\frac{1}{2}}(\theta). \quad (2.24)$$

It is readily verified that the convexity condition for this curve reduces to (2.23) where k is again defined by (2.15). The planar curve (2.24) can be thought of as the projection of (2.18) into a two-dimensional plane with $\mathbf{i}$ aligned along the cone axis.

The condition (2.23) can be converted to a local convexity condition by taking $\theta^*-\theta$ to be small, by making a Taylor series expansion of f about θ, and by retaining only the terms of order $(\theta^*-\theta)^2$ in (2.23). The result, expressed in three ways, is

$$2ff''+4f^2-f'^2=4f^{3/2}[(f^{\frac{1}{2}})''+f^{\frac{1}{2}}]=4f^2[1+k^2-k']\geqslant 0. \quad (2.25)$$

Satisfaction of (2.25) for all θ is necessary and sufficient for satisfaction of (2.23) if f and f' are continuous at any point where f'' is discontinuous.

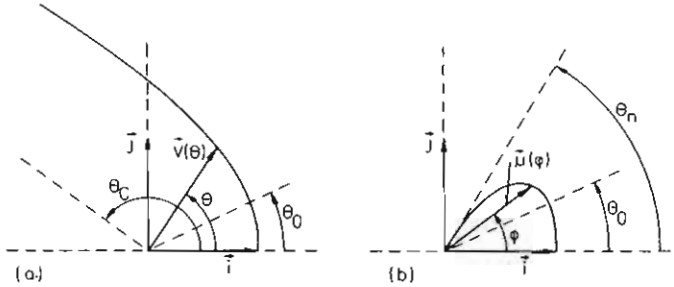

FIG. 3. (a) Projection of surface $W^p=\frac{1}{2}$ in stress-rate space; (b) projection of surface $W^p=\frac{1}{2}$ in strain-rate space.

A simple choice for $f(\theta)$ which satisfies (2.22) and (2.25) is

$$f = \begin{cases} 1, & 0 \leqslant \theta \leqslant \theta_0, \\ \cos^2\left[\frac{\pi}{2}\left(\frac{\theta-\theta_0}{\theta_c-\theta_0}\right)\right], & \theta_0 \leqslant \theta \leqslant \theta_c, \\ 0, & \theta_c \leqslant \theta \leqslant \pi, \end{cases} \tag{2.26}$$

with

$$k = \begin{cases} 0, & 0 \leqslant \theta \leqslant \theta_c, \\ \frac{\frac{1}{2}\pi}{(\theta_c-\theta_0)} \tan\left[\frac{1}{2}\pi\left(\frac{\theta-\theta_0}{\theta_c-\theta_0}\right)\right], & \theta_0 \leqslant \theta \leqslant \theta_c, \\ 0, & \theta_c \leqslant \theta \leqslant \pi, \end{cases} \tag{2.27}$$

and with $\theta_0 \leqslant \theta_c - \frac{1}{2}\pi$. Both f and f' are continuous at θ_0 and at θ_c. From (2.14) it can be seen that continuity of ε^p at θ_0 and θ_c is insured by continuity of f and f'. The curve determined by (2.26) is that depicted in Fig. 3(a). In the total loading range the curve coincides with a unit circle. Since $f''(\theta_0) \neq 0$ as $\theta_0 \to 0$, (2.26) does not provide a thoroughly nonlinear relation with plastic compliances $\mathbf{C}$ for $\theta \approx 0$.

2.4 *Instantaneous compliances*

The instantaneous compliance tensor $\mathbf{M}$ relates the strain-rate and the stress-rate by

$$\dot{\boldsymbol{\varepsilon}} = \mathbf{M}\dot{\boldsymbol{\sigma}}, \tag{2.28}$$

The compliance tensor is not unique since, for example, any fourth-order tensor of the form $\mathbf{a} \otimes \mathbf{a}$, where $\mathbf{a}$ is a symmetric deviator tensor orthogonal to $\dot{\boldsymbol{\sigma}}$, can be added to $\mathbf{M}$ without altering $\dot{\boldsymbol{\varepsilon}}$. Nevertheless, since $W = W^e + W^p$ is strictly convex, we are assured that the choice

$$\mathbf{M} = \frac{\partial^2 W}{\partial\dot{\boldsymbol{\sigma}}\partial\dot{\boldsymbol{\sigma}}} = \mathscr{M} + \frac{\partial^2 W^p}{\partial\dot{\boldsymbol{\sigma}}\partial\dot{\boldsymbol{\sigma}}} \tag{2.29}$$

is always positive definite. The calculation in (2.29) using (2.9) is somewhat lengthy but the details need not be given here. The result is

$$\mathbf{M} = \mathscr{M} + f\mathbf{C} + \tfrac{1}{2}f'[\cot\theta(\mathbf{C} - \mathbf{p}\otimes\mathbf{p} - \mathbf{q}\otimes\mathbf{q}) + \mathbf{H}] + \tfrac{1}{2}f''\mathbf{q}\otimes\mathbf{q}, \tag{2.30}$$

where

$$\mathbf{p} = \mathbf{C}\dot{\boldsymbol{\sigma}}/(\mathbf{C}\dot{\boldsymbol{\sigma}}\dot{\boldsymbol{\sigma}})^{\frac{1}{2}} \quad \text{and} \quad \mathbf{q} = (\tan\theta)^{-1}\mathbf{p} - (\sin\theta)^{-1}\boldsymbol{\mu} \tag{2.31}$$

and the Cartesian components of $\mathbf{H}$ are

$$H_{ijkl} = p_{ij}q_{kl} + p_{kl}q_{ij}.$$

In the total loading range, $\mathbf{M} = \mathscr{M} + \mathbf{C}$, as expected, and in the elastic unloading range, $\mathbf{M} = \mathscr{M}$. A discontinuity in f'' implies a discontinuity in $\mathbf{M}$, but the strain-rate is necessarily a continuous function of $\dot{\boldsymbol{\sigma}}$ as long as f and f' are continuous, as

previously shown. If $\theta_0 = 0$, corresponding to thoroughly nonlinear behavior, $\mathbf{M}$ will approach $\mathscr{M} + \mathbf{C}$ in the neighborhood of $\theta = 0$ if $f''(0) = 0$ with $f(0) = 1$ and $f'(0) = 0$.

2.5 *Inversion of relation between* $\boldsymbol{\varepsilon}^p$ *and* $\dot{\boldsymbol{\sigma}}$

An inverted relation expressing the stress-rate in terms of the plastic strain-rate is not useful in itself unless the elastic strain-rate is neglected. Nevertheless, the material in this sub-section adds to the understanding of several notions, including the precise meaning of the "forward cone of normals" in the present context. An alternative way of specifying the transition function also emerges.

Let $\mathbf{D}$ be the inverse of $\mathbf{C}$ in the sense that $\mathbf{D}$ shares the same indicial symmetries as $\mathbf{C}$ and also satisfies $\mathbf{DC} = \mathbf{CD} = \bar{\mathbf{I}}$, where $\bar{\mathbf{I}}$ is the special identity tensor whose Cartesian components are

$$\bar{I}_{ijkl} = \tfrac{1}{2}(\delta_{ik}\delta_{jl} + \delta_{il}\delta_{jk}) - \tfrac{1}{3}\delta_{ij}\delta_{kl}. \tag{2.32}$$

Recall that $\boldsymbol{\mu} = \mathbf{C}\boldsymbol{\lambda}$ is the direction of the plastic strain-rate corresponding to a stress-rate directed along the axis of the cone in stress-rate space. Define a positive angle ϕ of the direction of $\boldsymbol{\varepsilon}^p$ measured from $\boldsymbol{\mu}$ according to the dual of (2.13) as

$$\cos\phi = \frac{\mathbf{D}\boldsymbol{\mu}\boldsymbol{\varepsilon}^p}{(\mathbf{D}\boldsymbol{\varepsilon}^p\boldsymbol{\varepsilon}^p)^{\frac{1}{2}}} = \frac{\boldsymbol{\lambda}\boldsymbol{\varepsilon}^p}{(\mathbf{D}\boldsymbol{\varepsilon}^p\boldsymbol{\varepsilon}^p)^{\frac{1}{2}}}. \tag{2.33}$$

where $\boldsymbol{\lambda} = \mathbf{D}\boldsymbol{\mu}$. A direct calculation using (2.14) gives

$$\mathbf{D}\boldsymbol{\varepsilon}^p\boldsymbol{\varepsilon}^p = f^2[1 + k^2]\mathbf{C}\dot{\boldsymbol{\sigma}}\dot{\boldsymbol{\sigma}}. \tag{2.34}$$

Further reduction of (2.33) using (2.14) and the definition of $\cos\theta$ provides the following expression for ϕ in terms of θ alone

$$\cos\phi = \frac{1 + k(\theta)\tan\theta}{[1 + k^2(\theta)]^{\frac{1}{2}}}\cos\theta, \tag{2.35}$$

This expression can be reduced still further to the simple connection

$$\tan(\theta - \phi) = k(\theta). \tag{2.36}$$

From (2.36) it can be seen that $\phi = \theta$ in the total loading range and, in particular, $\phi = \theta_0$ for $\theta = \theta_0$. From (2.36) it can also readily be shown that

$$\frac{d\phi}{d\theta} = \frac{1 + k^2 - k'}{1 + k^2} \geqslant 0, \tag{2.37}$$

where the inequality is a consequence of convexity from (2.25). Thus, ϕ increases monotonically with θ. Since $k \to +\infty$ as $\theta \to \theta_c$, it follows from (2.36) that $\phi \to \theta_c - \frac{1}{2}\pi$ as $\theta \to \theta_c$. The so-called forward cone of normals which contains the plastic strain-rate is therefore specified by $\phi \leqslant \theta_n$ where

$$\theta_n = \theta_c - \tfrac{1}{2}\pi. \tag{2.38}$$

These features are depicted in Fig. 2(b).

We now regard $W^p = \frac{1}{2}\dot{\boldsymbol{\sigma}}\boldsymbol{\varepsilon}^p$ as a function of $\boldsymbol{\varepsilon}^p$. As a result of (2.34) and the fact that ϕ is a function of θ alone, (2.9) can be written as

$$W^p = \tfrac{1}{2}g(\phi)\mathbf{D}\boldsymbol{\varepsilon}^p\boldsymbol{\varepsilon}^p, \tag{2.39}$$

where

$$f(\theta)g(\phi) = [1+k^2(\theta)]^{-1}. \tag{2.40}$$

The inverted expression for the deviatoric part of $\dot{\boldsymbol{\sigma}}$, $\dot{\mathbf{s}} = \partial W^p/\partial\boldsymbol{\varepsilon}^p$, is

$$\dot{\mathbf{s}} = g(\phi)[(1+l(\phi)\cot\phi)\mathbf{D} - l(\phi)(\sin\phi\cos\phi)^{-1}\boldsymbol{\lambda}\otimes\boldsymbol{\lambda}]\boldsymbol{\varepsilon}^p, \tag{2.41}$$

where

$$l(\phi) = \tfrac{1}{2}g'/g = (\ln g^{\frac{1}{2}})'. \tag{2.42}$$

Furthermore, it is a straightforward matter to show that

$$l(\phi) = k(\theta). \tag{2.43}$$

The duality between the two sets of equations enables one to assert immediately that convexity of W^p with respect to $\boldsymbol{\varepsilon}^p$ reduces to the condition for the convexity of the planar curve

$$\mathbf{u}(\phi) = (\cos\phi\,\mathbf{i} + \sin\phi\,\mathbf{j})/g^{\frac{1}{2}}(\phi) \tag{2.44}$$

together with the side condition $1 + l(\phi)\cot\phi \geqslant 0$. Convexity of (2.44) is ensured by

$$2gg'' + 4g^2 - g'^2 = 4g^{3/2}[g^{\frac{1}{2}\prime\prime} + g^{\frac{1}{2}}] = 4g^2[1 + l^2 + l'] \geqslant 0 \tag{2.45}$$

together with the continuity of g and g'. Satisfaction of either one of (2.25) or (2.45) ensures satisfaction of the other when f and g are linked by (2.40) It can also be shown that $\mathbf{v}(\theta)$ is the outward normal to the curve $\mathbf{u}(\phi)$, and *vice versa*, with arctan k as the angle between $\mathbf{u}$ and $\mathbf{v}$.

An alternative transition function to (2.26) which satisfies (2.45) and the side condition is

$$g(\phi) = \begin{cases} 1, & 0 \leqslant \phi \leqslant \theta_0, \\ (1-x^m)^{-2}, & \theta_0 \leqslant \phi \leqslant \theta_n, \end{cases} \tag{2.46}$$

with

$$l(\phi) = \begin{cases} 0, & 0 \leqslant \phi \leqslant \theta_0, \\ \dfrac{mx^{m-1}}{(\theta_n-\theta_0)(1-x^m)}, & \theta_0 \leqslant \phi \leqslant \theta_n, \end{cases} \tag{2.47}$$

where $x = (\phi-\theta_0)/(\theta_n-\theta_0)$ and $m \geqslant 2$. If $m > 2$, $g'' = 0$ continuously at $\phi = \theta_0$. Thus, (2.46) supplies a thoroughly nonlinear relation with $\theta_0 = 0$ if $m > 2$. A typical member of (2.46) is depicted as $\mathbf{u}(\phi)$ in Fig. 3(b).

3. J_2 Corner theory

The general framework of Section 2 will now be specialized to what is probably the simplest meaningful version of the theory. Attention will continue to be directed to the small strain regime, but possible "finite strain" extensions will be mentioned.

The specialization follows almost immediately from the previous development. It is constructed to coincide with J_2 deformation theory for total loading histories for which θ is always less than θ_0. This means that the relation is integrable with limited path-independence for such histories. Of course, for strictly proportional loading histories, the present theory, J_2 deformation theory and J_2 flow theory all coincide. The theory can be regarded as an extension of BUDIANSKY's (1959) treatment of total loading based on J_2 deformation theory.

3.1 *Small strain version*

Using Cartesian components, let

$$s_{ij} = \sigma_{ij} - \tfrac{1}{3}\sigma_{kk}\delta_{ij}$$

be the stress deviator and introduce the effective stress

$$\sigma_e^2 = 3J_2 = \tfrac{3}{2}s_{ij}s_{ij}. \tag{3.1}$$

In incremental form, J_2 deformation theory has the form

$$\dot{\varepsilon}_{ij} = \mathscr{M}_{ijkl}\dot{\sigma}_{kl} + C_{ijkl}\dot{\sigma}_{kl}, \tag{3.2}$$

where

$$\mathscr{M}_{ijkl} = \frac{1}{2G}\bar{I}_{ijkl} + \frac{1-2\nu}{3E}\delta_{ij}\delta_{kl} \tag{3.3}$$

and

$$C_{ijkl} = \frac{3}{2}\left[\left(\frac{1}{E_s} - \frac{1}{E}\right)\bar{I}_{ijkl} + \frac{3}{2}\left(\frac{1}{E_t} - \frac{1}{E_s}\right)\frac{s_{ij}s_{kl}}{\sigma_e^2}\right]. \tag{3.4}$$

Here, E is Young's modulus, $G = E/2(1+\nu)$ is the elastic shear modulus, ν is Poisson's ratio and E_s and E_t are, respectively, the secant and tangent moduli of the uniaxial stress–strain curve at the current value of σ_e. The inverse of $\mathbf{C}$ as defined in Section 2 is

$$D_{ijkl} = \frac{E}{E-E_s}\left[\tfrac{2}{3}E_s\bar{I}_{ijkl} - \frac{E(E_s-E_t)}{(E-E_t)}\frac{s_{ij}s_{kl}}{\sigma_e^2}\right]. \tag{3.5}$$

The plastic total loading compliances in J_2 corner theory are taken to be $\mathbf{C}$ in (3.4) with elastic compliances as (3.3). The axis of the cone in stress-rate space is taken parallel to s_{ij}. From (2.11) and (2.12) it follows therefore that

$$\lambda_{ij} = \left(\frac{1}{E_t} - \frac{1}{E}\right)^{-\frac{1}{2}}\frac{s_{ij}}{\sigma_e} \quad \text{and} \quad \mu_{ij} = \frac{3}{2}\left(\frac{1}{E_t} - \frac{1}{E}\right)^{\frac{1}{2}}\frac{s_{ij}}{\sigma_e}. \tag{3.6}$$

Using the definition (2.13) gives

$$\cos\theta = \frac{\left(\frac{1}{E_t} - \frac{1}{E}\right)^{\frac{1}{2}}\dot{\sigma}_e}{\left[\frac{3}{2}\left(\frac{1}{E_s} - \frac{1}{E}\right)\dot{s}_{ij}\dot{s}_{ij} + \left(\frac{1}{E_t} - \frac{1}{E_s}\right)\dot{\sigma}_e^2\right]^{\frac{1}{2}}}, \tag{3.7}$$

where $\sigma_e \dot{\sigma}_e = (3/2) s_{ij} \dot{s}_{ij}$. A similar expression for $\cos \phi$ in terms of the plastic strain-rates can be derived. Written out, the potential of the stress-rate becomes

$$W(\dot{\sigma}) = \frac{1}{2}\left[\frac{1}{2G} + \frac{3}{2}\left(\frac{1}{E_s} - \frac{1}{E}\right) f(\theta)\right] \dot{s}_{ij}\dot{s}_{ij} + \frac{1}{2}\left(\frac{1}{E_t} - \frac{1}{E}\right) f(\theta)\dot{\sigma}_e^2 + \frac{1-2\nu}{6E}\dot{\sigma}_{kk}^2. \tag{3.8}$$

The expression for the plastic strain-rate (2.14) specializes directly.

We now introduce another angular measure of the stress-rate. Following BUDIANSKY (1959), let

$$\cos \beta = \frac{s_{ij}\dot{\sigma}_{ij}}{[(s_{kl}s_{kl})(\dot{s}_{pq}\dot{s}_{pq})]^{\frac{1}{2}}} = \frac{\dot{\sigma}_e}{[\frac{3}{2}\dot{s}_{ij}\dot{s}_{ij}]^{\frac{1}{2}}}. \tag{3.9}$$

Using (3.7) and (3.9) one can show that θ and β are simply related by

$$\tan \theta = a^{\frac{1}{2}} \tan \beta, \quad \text{where } a = \left(\frac{E}{E_s} - 1\right)\left(\frac{E}{E_t} - 1\right)^{-1}. \tag{3.10}$$

Furthermore, (3.8) can be re-expressed by eliminating $\dot{\sigma}_e$ using (3.9), with the result

$$W(\dot{\sigma}) = \frac{1}{4G} Q(\beta)\dot{s}_{ij}\dot{s}_{ij} + \frac{1-2\nu}{6E}\dot{\sigma}_{kk}^2, \tag{3.11}$$

where

$$Q(\beta) = 1 + 3G\left[\left(\frac{1}{E_t} - \frac{1}{E}\right)\cos^2 \beta + \left(\frac{1}{E_s} - \frac{1}{E}\right)\sin^2 \beta\right] f(\theta). \tag{3.12}$$

This form (3.11) for W, together with (3.9), is the specialization of CHRISTOFFERSEN's (1978) formulation for the case of isotropic elastic moduli.

The duality properties holding for this latter formulation involves the *total* strain-rate and its deviator, $\hat{\varepsilon}_{ij} = \varepsilon_{ij} - \frac{1}{3}\varepsilon_{pp}\delta_{ij}$. With

$$\cos \alpha = \frac{s_{ij}\dot{\varepsilon}_{ij}}{[(s_{kl}s_{kl})(\dot{\hat{\varepsilon}}_{pq}\dot{\hat{\varepsilon}}_{pq})]^{\frac{1}{2}}} \tag{3.13}$$

one can show (CHRISTOFFERSEN, 1978), analogous to (2.36), that

$$\tan(\beta - \alpha) = -\frac{1}{2}\frac{1}{Q}\frac{dQ}{d\beta} \equiv \tan \gamma \tag{3.14}$$

and

$$W(\varepsilon) = GP(\alpha)\hat{\varepsilon}_{ij}\hat{\varepsilon}_{ij} + \frac{E}{6(1-2\nu)}\varepsilon_{kk}^2, \tag{3.15}$$

where

$$P(\alpha)Q(\beta) = \cos^2 \gamma. \tag{3.16}$$

The counterpart to (2.43) is $Q^{-1}dQ/d\beta = -P^{-1}dP/d\alpha$.

The advantage of (3.15) is that it provides an explicit inverted relation between the stress-rate and the total strain-rate. The rate-equations from

$$\varepsilon = \partial W/\partial \dot{\sigma} \quad \text{and} \quad \dot{\sigma} = \partial W/\partial \varepsilon \tag{3.17}$$

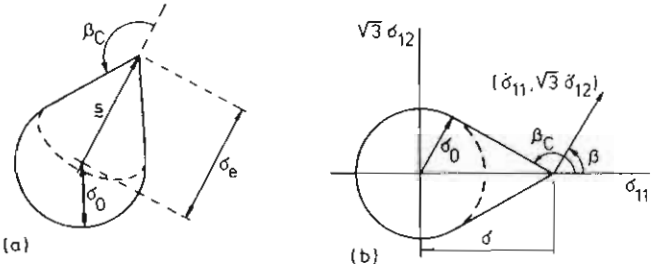

FIG. 4. (a) Yield surface in stress space; (b) projection of yield surface into plane of $(\sigma_{11}, \sqrt{3}\sigma_{12})$ following uniaxial stressing to $\sigma_{11} = \sigma$.

can be obtained, giving expressions similar to (2.14) and (2.41), but with ε replacing ε^p. Positive-definite compliances and moduli can be obtained as in Section 2.4. Further comments on the relation between the two formulations are given in the Appendix.

To complete the specification of J_2 corner theory it remains to specify the dependence of θ_c and θ_0 on σ_e and to select a transition function. The cone angle θ_c in stress-rate space can be related to the local conical yield surface in stress space. The simplest choice for a yield surface in stress space is that depicted in Fig. 4. It comprises an initial spherical surface $\sigma_e = \sigma_0$ and a conical surface of revolution about the axis between the origin and $\mathbf{s}$ such that the two surfaces meet with continuous tangents. Let $\mathbf{s}^*$ be any stress state on the conical surface in Fig. 4. That surface is specified by taking $\dot{\mathbf{s}} \propto \mathbf{s}^* - \mathbf{s}$ in (3.9) with $\beta = \beta_c$ where from the condition of continuous tangents,

$$\tan \beta_c = -\sigma_0/(\sigma_e^2 - \sigma_0^2)^{\frac{1}{2}}. \tag{3.18}$$

By (3.10),

$$\tan \theta_c = a^{\frac{1}{2}} \tan \beta_c. \tag{3.19}$$

For total loading histories to s, this yield surface is qualitatively in accord with yield surfaces from slip theory or from self-consistent models of polycrystals. The choice for θ_c from (3.19) and (3.10) also seems reasonable for more excursive stress histories such as those discussed in connection with Fig. 1. Other choices for θ_c in terms of σ_e may be prescribed. For example, in the sheet-necking problem treated in Section 4, elastic strains are neglected and θ_c is taken to be constant over the history.

To obtain some insight into the transition functions suppose that the material is stressed in uniaxial tension to $\sigma_{11} = \sigma$ and that the only non-zero stress-rate components from this state are $\dot{\sigma}_{11}$ and $\dot{\sigma}_{12}$ as shown in Fig. 4(b). The angle θ from (3.7) is given by

$$\cos \theta = \dot{\sigma}_{11}/(\dot{\sigma}_{11}^2 + 3a\dot{\sigma}_{12}^2)^{\frac{1}{2}} \quad \text{or} \quad \tan \theta = (3a)^{\frac{1}{2}}|\dot{\sigma}_{12}|/\dot{\sigma}_{11}. \tag{3.20}$$

Define an instantaneous effective shear modulus as $G_e = \dot{\sigma}_{12}/(2\dot{\varepsilon}_{12})$. Using (2.14) and the associated equations (3.4) and (3.6) to calculate $\dot{\varepsilon}_{12}$ for arbitrary $\dot{\sigma}_{11}$ and $\dot{\sigma}_{12}$, we find

$$\frac{G}{G_e} = 1 + \frac{3}{2(1+\nu)}\left(\frac{E}{E_s} - 1\right)(1 - k(\theta)\cot\theta) f(\theta). \tag{3.21}$$

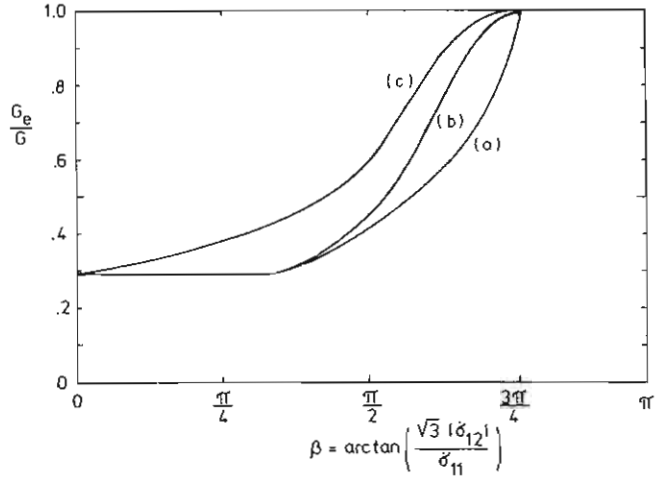

FIG. 5. Instantaneous effective shear modulus, $G_e = \dot{\sigma}_{12}/(2\dot{\varepsilon}_{12})$, following uniaxial stressing. See text for specification of parameters. Curve (a) is based on $f(\theta)$ with $\theta_0 = \frac{1}{2}\theta_n$; curve (b) is based on $g(\phi)$ with $\theta_0 = \frac{1}{2}\theta_n$; the curve (c) is a thoroughly nonlinear characterization using $g(\phi)$ with $\theta_0 = 0$.

The convexity condition (2.22) ensures that $G_e \leqslant G$ if $E_s \leqslant E$. Alternatively, G_e can be expressed in terms of $g(\phi)$ using (2.41) instead of (2.14) with the result

$$\frac{G}{G_e} = 1 + \frac{3}{2(1+\nu)}\left(\frac{E}{E_s} - 1\right)\frac{1}{(1 + l(\phi)\cot\phi)g(\phi)}. \tag{3.22}$$

The dependence of G_e/G on $\beta = \arctan(\sqrt{3}|\dot{\sigma}_{12}|/\dot{\sigma}_{11})$ is shown in Fig. 5 for the two candidate transition functions, f in (2.26) and g in (2.46). To generate realistic values for a and E/E_s the Ramberg–Osgood uniaxial curve was assumed where

$$e = (\sigma/E) + (3/7)(\sigma/E)(\sigma/\sigma_0)^{n-1}. \tag{3.23}$$

For this curve, $a = 1/n$. For the plots in Fig. 5, $\nu = 1/3$, $n = 5$ and $\sigma = 1.5\sigma_0$. From (3.9) and (3.10), this gives $\beta_c = 138°$, $\theta_c = 158°$, and $\theta_n = 68°$. In the specification of f for curve (a), θ_0 was taken to be $\frac{1}{2}\theta_n$. In the specification of g, we took $m = 3$ with $\theta_0 = \frac{1}{2}\theta_n$ for curve (b) and $\theta_0 = 0$ for curve (c). (Recall that θ and ϕ are related by (2.36), and θ is related to β by (3.10).)

Curves similar to those in Fig. 5 were calculated using a self-consistent model of a polycrystal by HUTCHINSON (1970). Of the three curves in Fig. 5, (c) for the thoroughly nonlinear relation most closely duplicates the self-consistent results. Curve (a), based on f, is least like the self-consistent results because of the slow approach of G_e to G as $\beta \to \beta_c$.

3.2 *Extensions into the finite strain range*

Two possible extensions into the range when the stress levels become comparable in magnitude to the instantaneous moduli will be mentioned. The most straightforward one uses the above formulas unaltered with $\boldsymbol{\sigma}$ taken to be the Cauchy

stress and $\dot{\sigma}$ as its Jaumann rate. Cartesian components in the above equations may be converted to components referred to base vectors deforming with the material. Now, E_s and E_t are the secant and tangent moduli of the uniaxial true-stress–logarithmic-strain curve at σ_e. With this interpretation, the plastic total loading compliances (3.4) coincide with the proposal made by STÖREN and RICE (1975) in their theory for total loading increments.

In the finite strain range, the above proposal gives an integrable relation for total loading histories only when the principal axes of stress do not rotate relative to the material. Total loading is usually associated with the existence of limited path-independence, as in slip theory. Assuming that to be the case, a total loading history of an initially isotropic elastic–plastic solid should coincide with a corresponding history in an isotropic nonlinear elastic solid, in the same manner as elucidated by SANDERS (1954) for the small strain range. An alternative proposal is to employ a finite strain J_2 deformation theory (i.e. a true nonlinear elastic relation such as that suggested by HUTCHINSON and NEALE (1978)) to generate the instantaneous total loading compliances. In principal stress axes, the normal components of $\mathbf{C}$, e.g. C_{1111}, C_{1122}, etc., are the same as those in (3.4) but the shearing components, e.g. C_{1212}, are not given by (3.4) in the finite-strain range. General expressions for these latter components have been given by BIOT (1965) and HILL (1970) for nonlinear isotropic elastic solids.

When the material is elastically compressible the above two proposals cannot be used in the standard variational principle for the incremental boundary-value problem (HILL, 1961). A simple remedy is to replace the Cauchy stress by the Kirchhoff stress in the above formulas, similar to what has been discussed elsewhere. This interchange makes little difference as long as the elastic volume change is small.

4. APPLICATION OF J_2 CORNER THEORY TO SHEET NECKING

The approach of MARCINIAK and KUCZYŃSKI (1967) will be applied to calculate the development of a necking band in a thin sheet subject to biaxial stretching in its plane. This approach neglects 3-dimensional aspects of the stress and strain fields which become especially important in the final stages of necking. Plane stress conditions are

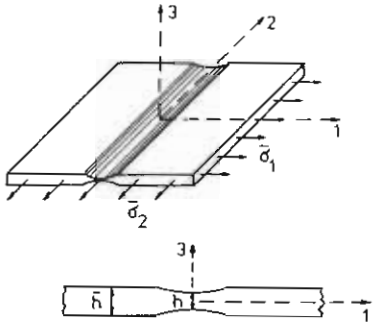

FIG. 6. Sheet geometry.

assumed. This permits the behavior at the minimum point of the infinitely long band (see Fig. 6) to be related directly to the deformation imposed on the uniform sections of the sheet outside the band. With $\bar{e}_1$ and $\bar{e}_2$ as the principal logarithmic strains in the uniform sections, a proportional straining history is imposed such that

$$\bar{e}_2 = \rho \bar{e}_1, \tag{4.1}$$

where ρ is fixed and $\bar{e}_1$ is monotonically increased. Attention will be restricted to the range $0 \leqslant \rho \leqslant 1$ for which a band aligned with the 2-axis is most critical.

The two nonzero, true stress components are σ_1 and σ_2. No rotation of the principal stress axes occurs and thus the two finite strain versions of J_2 corner theory discussed in Section 3 coincide.† Elastic strains are neglected. The material is incompressible and is assumed to be characterized by J_2 corner theory with $E \to \infty$ in the appropriate formulas. When specialized to plane stress with $\sigma_{12} = \dot{\sigma}_{12} = 0$, the inverted relation (2.41) can be reduced to

$$\left.\begin{aligned} \dot{\sigma}_1 &= L_{11}(\phi)\dot{\varepsilon}_1 + L_{12}(\phi)\dot{\varepsilon}_2, \\ \dot{\sigma}_2 &= L_{12}(\phi)\dot{\varepsilon}_1 + L_{22}(\phi)\dot{\varepsilon}_2, \end{aligned}\right\} \tag{4.2}$$

wherein the third equation expressing $\dot{\sigma}_3 = 0$ has been used. Here,

$$L_{\alpha\beta} = g[(1 + l\cot\phi)L^0_{\alpha\beta} - l(\sin\phi\cos\phi)^{-1}E_t\sigma_\alpha\sigma_\beta\sigma_e^{-2}] \tag{4.3}$$

for $\alpha = 1, 2$ and $\beta = 1, 2$. The plane stress total loading moduli (the plane stress specialization of $\mathbf{D}$) are

$$L^0_{\alpha\beta} = \tfrac{2}{3}(1 + \delta_{\alpha\beta})E_s - (E_s - E_t)\sigma_\alpha\sigma_\beta\sigma_e^{-2}, \tag{4.4}$$

where $\delta_{\alpha\beta} = 1$ for $\alpha = \beta$ and zero otherwise.

The expression for $\cos\phi$ in (2.33) reduces to

$$\cos\phi = \frac{E_t^{\frac{1}{2}}(\sigma_1\dot{\varepsilon}_1 + \sigma_2\dot{\varepsilon}_2)}{[\tfrac{4}{3}E_s\sigma_e^2(\dot{\varepsilon}_1^2 + \dot{\varepsilon}_2^2 + \dot{\varepsilon}_1\dot{\varepsilon}_2) - (E_s - E_t)(\sigma_1\dot{\varepsilon}_1 + \sigma_2\dot{\varepsilon}_2)^2]^{\frac{1}{2}}}. \tag{4.5}$$

The functions $g(\phi)$ and $l(\phi)$ will be taken as (2.46) and (2.47). A pure power relation is assumed between the true stress and natural strain in uniaxial tension according to

$$\sigma = Ke^N \tag{4.6}$$

so that

$$E_t = NE_s = NK(\sigma_e/K)^{1-1/N}, \tag{4.7}$$

where

$$\sigma_e = (\sigma_1^2 + \sigma_2^2 - \sigma_1\sigma_2)^{\frac{1}{2}}. \tag{4.8}$$

In the uniform sections of the sheet, and everywhere in the perfect sheet prior to bifurcation, the straining is proportional ($\phi = 0$). Then the stresses from (4.2) in terms of $\bar{e}_1$ are the same as in the analysis of MARCINIAK and KUCZYŃSKI (1967) who

† The bifurcation strain (4.15) given below holds for all $N \leqslant 1$ for moduli $\mathbf{D}$ derived from the true finite strain deformation theory. For moduli $\mathbf{D}$ given by (3.5), out-of-plane shear band modes intercede prior to the plane stress bifurcation mode associated with (4.15) in the upper range of N-values (e.g. for $N > 1/3$ when $\rho = 1$), as discussed by HUTCHINSON (1979).

used flow theory. With bars denoting quantities in the uniform sections, these stresses are

$$\left.\begin{aligned}(\bar{\sigma}_e/K)^{1/N} &= 2(1+\rho+\rho^2)^{\frac{1}{2}}\bar{e}_1/\sqrt{3},\\ \bar{\sigma}_1 &= (2+\rho)[3(1+\rho+\rho^2)]^{-\frac{1}{2}}\bar{\sigma}_e,\\ \bar{\sigma}_2 &= (1+2\rho)[3(1+\rho+\rho^2)]^{-\frac{1}{2}}\bar{\sigma}_e.\end{aligned}\right\} \tag{4.9}$$

Logarithmic strains at the minimum section of the neck are denoted by e_1 and e_2, true stresses by σ_1 and σ_2, strain-rates by $\varepsilon_1 = \dot{e}_1$ and $\varepsilon_2 = \dot{e}_2$, and the thickness by h. In the uniform sections the thickness is $\bar{h}$. The initial thickness imperfection is specified in terms of the thicknesses prior to any straining, h_i and $\bar{h}_i$, by

$$\xi = (\bar{h}_i - h_i)/\bar{h}_i \geqslant 0. \tag{4.10}$$

Equilibrium in the 1-direction requires $\sigma_1 h = \bar{\sigma}_1 \bar{h}$ or

$$\dot{\sigma}_1 h + \sigma_1 \dot{h} = \dot{\bar{\sigma}}_1 \bar{h} + \bar{\sigma}_1 \dot{\bar{h}}. \tag{4.11}$$

In the 2-direction, the geometric constraint $e_2 = \bar{e}_2$ holds so that

$$\varepsilon_2 = \bar{\varepsilon}_2 = \rho\bar{\varepsilon}_1. \tag{4.12}$$

To obtain the relation between ε_1 in the neck and $\bar{\varepsilon}_1$ imposed on the uniform sections, use the constitutive law (4.2) to eliminate $\dot{\sigma}_1$ in (4.11), noting $\sigma_1 = \bar{h}\bar{\sigma}_1/h$ and $\dot{h}/h = \varepsilon_3 = -(\varepsilon_1 + \varepsilon_2)$. In addition, use the total loading moduli (4.4) together with (4.9) to eliminate $\dot{\bar{\sigma}}_1$. The result is

$$[L_{11}(\phi) - \sigma_1]\varepsilon_1 = [A - \rho L_{12}(\phi)]\bar{\varepsilon}_1, \tag{4.13}$$

where

$$A = (\bar{h}/h)[2(2+\rho)N\bar{E}_s/3 - \bar{\sigma}_1]. \tag{4.14}$$

Equation (4.13) is supplemented by (4.2), (4.5) and (4.12). The initial condition is (4.10).

Bifurcation can first occur in the initially perfect sheet ($\xi = 0$) at the lowest value of $\bar{e}_1$ for which (4.13) admits a solution different from $\varepsilon_1 = \bar{\varepsilon}_1$. Bifurcation occurs when $\bar{\sigma}_1 = L_{11}(\phi)$ (or, equivalently, $A = \rho L_{12}(\phi)$). The lowest bifurcation mode must satisfy the total loading condition $\phi \leqslant \theta_0$ so that $L_{11} = L^0_{11}$.† Solving for the bifurcation strain $\bar{e}^c_1$ from $\bar{\sigma}_1 = L^0_{11}$, using (4.4), (4.8) and (4.9), gives STÖREN and RICE's (1975) formula

$$\bar{e}^c_1 = \frac{3\rho^2 + N(2+\rho)^2}{2(2+\rho)(1+\rho+\rho^2)}. \tag{4.15}$$

Below some detailed numerical results for imperfect sheets will be shown for the case $\rho = 1$; then,

$$\bar{e}^c_1 = (1+3N)/6. \tag{4.16}$$

† This is the generalized Shanley condition. HILL's (1961) sufficiency condition for uniqueness requires the introduction of a set of comparison moduli in a quadratic bifurcation functional. We mention in passing that, with **D** taken as the comparison moduli, application of the condition using corner theory with elastic strains neglected requires that $\frac{1}{2}(g-1)\mathbf{D}\boldsymbol{\varepsilon}\boldsymbol{\varepsilon}$ be convex. For the g given by (2.46), this can be established directly simply by replacing g by $g-1$ in (2.45).

In order to understand the behavior immediately following bifurcation consider first a sheet of nonlinear elastic material specified by the instantaneous moduli $L^0_{\alpha\beta}$ in (4.4). If it turns out that this material everywhere satisfies $\phi \leqslant \theta_0$ in some finite neighborhood of the bifurcation point, then its behavior will necessarily coincide with that of the plastic sheet. But, usually, the bifurcation mode of the nonlinear elastic sheet violates $\phi \leqslant \theta_0$ in portions of the sheet, and this is the case in the examples studied here. Then, the bifurcation mode for the plastic sheet must satisfy $\phi = \theta_0$ at at least one point with $\phi \leqslant \theta_0$ elsewhere. That is, the stiffening effect associated with plastic increments falling outside of the total loading range must *start* at bifureation. Otherwise, by continuity, the behavior would coincide initially with that of the nonlinear elastic sheet in contradiction to our assumption.

The bifurcation mode is the linear combination of the fundamental uniform solution plus the eigenmode. Let $R = \varepsilon_1/\bar{\varepsilon}_1$ in the bifurcation mode. Enforcing the condition $\phi = \theta_0$ in the neck using (4.5) gives, after some algebraic simplification,

$$R = \frac{3\rho\cos^2\theta_0 - N\rho(1+2\rho)^2\sin^2\theta_0}{3\rho\cos^2\theta_0 + N(2+\rho)(1+2\rho)\sin^2\theta_0 - (3N)^{\frac{1}{2}}(1+\rho+\rho^2)\sin 2\theta_0}. \tag{4.17}$$

The initial slope of $e_1/\bar{e}_1$ following bifurcation, which will be displayed below in a figure, is

$$\frac{d}{d\bar{e}_1}\left(\frac{e_1}{\bar{e}_1}\right) = \frac{R-1}{\bar{e}_1^c}. \tag{4.18}$$

Numerical calculations have been carried out to obtain the relation between e_1 and $\bar{e}_1$ in the imperfect sheet. These are inherently incremental calculations using (4.13) and the associated equations. Small increments in $\varepsilon_1 = \dot{e}_1$ were specified and the increment in $\bar{\varepsilon}_1 = \dot{\bar{e}}_1$ and other quantities were computed. Equations (4.5) and (4.13), with (4.12), can be regarded as a pair of simultaneous equations for ϕ and $\varepsilon_1/\bar{\varepsilon}_1$. The results shown in the figures to follow were obtained by solving this pair of equations numerically at each incremental step. A much simpler scheme was also tried which used the ϕ-value from the previous step in (4.13) in the current step. This method required no iteration to obtain ϕ and was successful as long as the step-size was very small where ϕ was changing rapidly. A scheme such as this would be the simplest to implement in large numerical calculations using, for example, a finite element method. The efficiency and stability of various solution methods will require further study.

The development of the strain in the neck e_1 relative to the strain outside the neck $\bar{e}_1$ is illustrated for several cases in Fig. 7. In all four plots, $\rho = 1$ and $N = 0.2$. For reference, curves for the nonlinear elastic sheet, with $L_{\alpha\beta} = L^0_{\alpha\beta}$ for all ϕ, are shown in Fig. 7(a). Three different choices of parameters in the specification of $g(\phi)$ in (2.46) have been made for the results in Fig. 7(b–d). In each case, $m = 3$ and θ_c is taken to be constant. By (3.19), β_c is also constant since $a = N$. Fig. 7(b) displays the response when the corner is rather sharp with a substantial total loading range ($\theta_c = 135°$, $\theta_n = 45°$, $\theta_0 = \frac{1}{2}\theta_n$), while in Fig. 7(c), by contrast, the corner is not nearly so sharp ($\theta_c = 115°$, $\theta_n = 25°$, $\theta_0 = \frac{1}{2}\theta_n$). The sheet material in Fig. 7(d) is thoroughly nonlinear ($\theta_c = 135°$, $\theta_n = 45°$, $\theta_n = 0$).

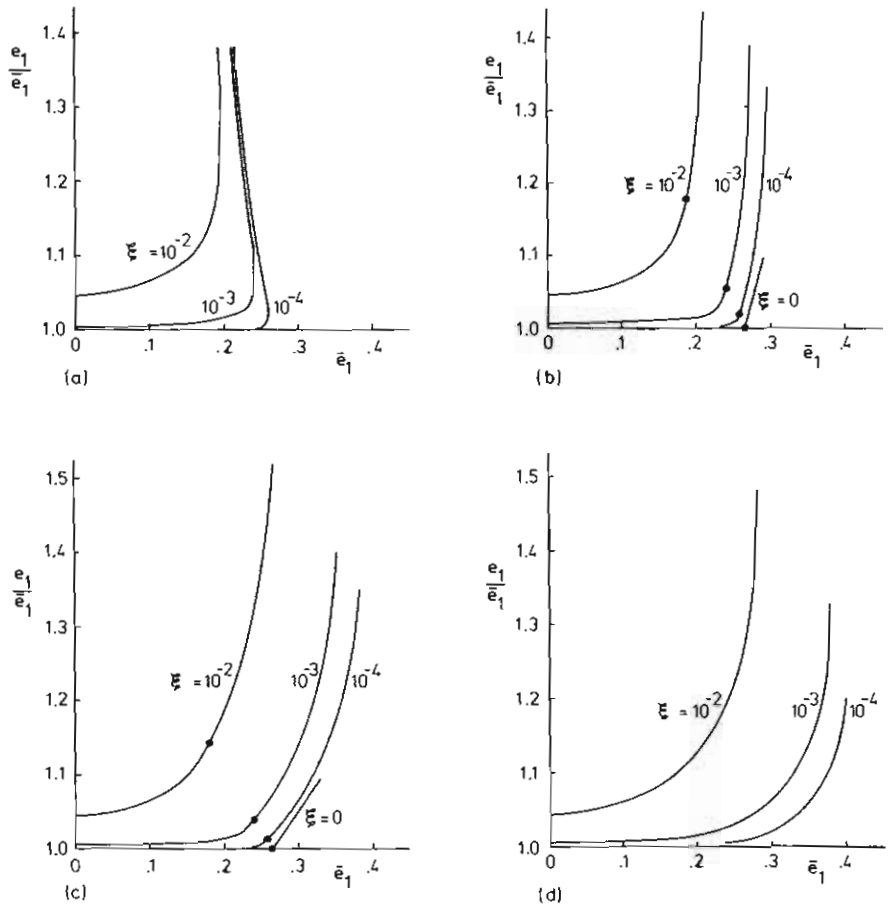

FIG. 7. Ratio of strain in neck to strain outside of neck, $e_1/\bar{e}_1$, as a function of strain outside of neck. In all cases, $N = 0.2$ and $\rho = 1$. (a) Nonlinear elastic sheet; (b) $\theta_n = 45°$, $\theta_0 = 22.5°$; (c) $\theta_n = 25°$; $\theta_0 = 12.5°$; and (d) $\theta_n = 45°$, $\theta_0 = 0°$. Only the initial slope is shown for the perfect sheet ($\xi = 0$). Curves for the imperfect plastic sheets are terminated when $(\bar{e}_1)_{max}$ is attained.

The solid dots on the curves in Fig. 7(b, c) mark the first point in the history where the material response in the neck passes out of the total loading range, that is, where $\phi = \theta_0$. The full response of the perfect sheet ($\xi = 0$) has not been computed, but the initial slope from (4.18) is shown. In the case of the thoroughly nonlinear sheet material in Fig. 7(d), this initial slope is necessarily zero since $R \to 1$ as $\theta_0 \to 0$.

Curves of ϕ for the neck material as a function of e_1 are shown in Fig. 8 for the sheet of Fig. 7. At low e_1, the response is essentially proportional with $\phi \approx 0$. As the neck develops, ϕ grows rapidly. The material in the neck must make the transition from essentially equal biaxial stretching at low e_1 ($\varepsilon_1 = \varepsilon_2 = -\frac{1}{2}\varepsilon_3$) to a state of in-plane plane strain ($\varepsilon_3 = -\varepsilon_1$, $\varepsilon_2 = 0$) in the fully developed neck. The curves for the plastic sheets have been terminated at the limit strain outside the neck, $(\bar{e}_1)_{max}$. Had

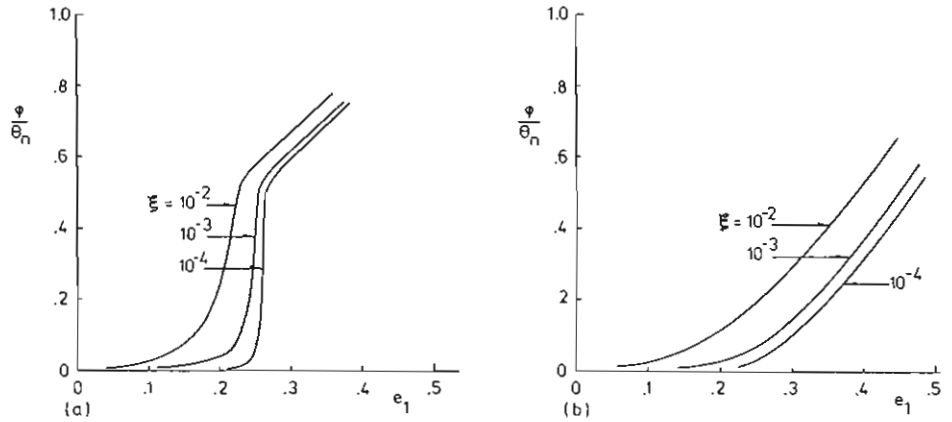

FIG. 8. History of ϕ in neck as a function of strain in neck, e_1. Plots are terminated at attainment of limit strain outside neck. (a) Case (b) of Fig. 7; $\theta_n = 45°$, $\theta_0 = 22.5°$. (b) Case (d) of Fig. 7; $\theta_n = 45°$, $\theta_0 = 0°$.

they been continued further, ϕ would attain a maximum and then approach zero as the limiting state of in-plane plane strain is approached.

Some dependence of the limit strains on the form of the transition function $g(\phi)$ is to be expected. It must be remembered that the bifurcation strain predicted on the basis of the corresponding flow theory (J_2 flow theory) is infinite with an associated unrealistic imperfection-sensitivity. Viewed from this perspective, the differences in the responses in Fig. 7(b–d) are not large, considering the significant differences between the choices for $g(\phi)$.

ACKNOWLEDGEMENT

The first stages of the work of J. W. H. was supported in part by the U.S. National Science Foundation under Grant ENG78-10756 and by the Division of Applied Sciences, Harvard University; and the later stages were completed while he was visiting at, and supported by, the Department of Solid Mechanics of The Technical University of Denmark.

REFERENCES

BATDORF, S. B. 1949 *J. Aero. Sci.* **16,** 405.

BATDORF, S. B. and BUDIANSKY, B. 1949 *A mathematical theory of plasticity based on the concept of slip*. NACA TN No. 1871.

BIOT, M. A. 1965 *Mechanics of Incremental Deformation*, p. 92. Wiley, New York.

BUDIANSKY, B. 1959 *Trans. ASME* **81,** Series E, *J. appl. Mech.* **26,** 259.

CHRISTOFFERSEN, J. 1978 *A simple convex stress rate–strain rate relation in plasticity not relying on the yield surface concept*. Report No. 147, Danish Center for Applied Mathematics and Mechanics, Technical University of Denmark, Lyngby.

HECKER, S. S.	1976	*Constitutive Equations in Viscoplasticity: Computational and Engineering Aspects,* AMD Vol. 20, (edited by J. A. Stricklin and K. J. Saczalski), p. 1. American Society of Mechanical Engineers, New York.
HILL, R.	1961	*Problems of Continuum Mechanics,* (Contributions in Honor of the Seventieth Birthday of Academician N. I. Muskhelishvili, 16th February 1961; edited by M. A. Lavrentev *et al.*), (English edition edited by J. R. M. Radok), p. 155. Society for Industrial and Applied Mathematics, Philadelphia, PA.
	1966	*J. Mech. Phys. Solids* **14,** 95.
	1967	*Ibid.* **15,** 79.
	1970	*Proc. R. Soc. Lond. A* **314,** 457.
HUTCHINSON, J. W.	1970	*Ibid.* **319,** 247.
	1979	*Proceedings of the Eighth U.S. National Congress of Applied Mechanics,* (Los Angeles, June 1978), (edited by R. E. Kelly, p. 87. American Society of Mechanical Engineers, New York.
HUTCHINSON, J. W. and NEALE, K. W.	1978	*Mechanics of Sheet Metal Forming* (edited by D. P. Koistinen and N.-M. Wang), p. 127. Plenum Press, New York.
KOITER, W. T.	1953	*Q. appl. Math.* **11,** 350.
MANDEL, J.	1965	*Int. J. Solids Struct.* **1,** 273.
MARCINIAK, Z. and KUCZYŃSKI, K.	1967	*Int. J. Mech. Sci.,* **9,** 609.
SANDERS, Jr., J. L.	1954	*Proceedings of the Second U.S. National Congress of Applied Mechanics* (Ann Arbor, MI. 14–18 June 1954), (edited by P. M. Naghdi), p. 455. American Society of Mechanical Engineers, New York.
SEWELL, M. J.	1974	*J. Mech. Phys. Solids* **22,** 469.
SHANLEY, F. R.	1947	*J. Aero. Sci.* **14,** 261.
STÖREN, S. and RICE, J. R.	1975	*J. Mech. Phys. Solids* **23,** 421.
TVERGAARD, V.	1978	*Int. J. Mech. Sci.* **20,** 651.

APPENDIX

A COMPARISON OF THE TWO FORMS OF THE THEORY

With $\mathscr{M}$ as the instantaneous elastic compliances and $K = (\mathscr{M}\boldsymbol{\delta}\boldsymbol{\delta})^{-1}$ as the bulk modulus, let

$$\mathscr{M}' = \mathscr{M} - K^{-1}\boldsymbol{\kappa}\otimes\boldsymbol{\kappa} \quad \text{and} \quad \mathscr{M}'' = K^{-1}\boldsymbol{\kappa}\otimes\boldsymbol{\kappa}, \tag{A.1}$$

where $\boldsymbol{\kappa}$ has unit trace and is proportional to the elastic strain-rate produced by a hydrostatic stress-rate, $-\dot{p}\boldsymbol{\delta}$. CHRISTOFFERSEN's (1978) formulation of corner theory takes as the starting definitions,

$$W(\dot{\boldsymbol{\sigma}}) = \tfrac{1}{2}Q(\beta)\mathscr{M}'\dot{\boldsymbol{\sigma}}\dot{\boldsymbol{\sigma}} + \tfrac{1}{2}\mathscr{M}''\dot{\boldsymbol{\sigma}}\dot{\boldsymbol{\sigma}} \tag{A.2}$$

and

$$\cos\beta = \frac{\mathscr{M}'\boldsymbol{\lambda}\dot{\boldsymbol{\sigma}}}{(\mathscr{M}'\boldsymbol{\lambda}\boldsymbol{\lambda})^{\frac{1}{2}}(\mathscr{M}'\dot{\boldsymbol{\sigma}}\dot{\boldsymbol{\sigma}})^{\frac{1}{2}}}, \tag{A.3}$$

where for an isotropic elastic compliance tensor these equations reduce to (3.9) and (3.11) introduced earlier.

One can show that the formulation based on (A.2) and (A.3) is completely equivalent to that given in the body of the present paper based on (2.9) and (2.13) if the instantaneous plastic total loading compliances $\mathbf{C}$ can be expressed as a linear combination of $\mathscr{M}'$ and $\boldsymbol{\omega} \otimes \dot{\boldsymbol{\omega}}$, where $\boldsymbol{\omega} = \mathscr{M}'\boldsymbol{\lambda}$. This is the case for the small strain version of J_2 corner theory as has already been noted in Section 3. It also holds for the finite strain version when the total loading compliances (3.4) are used. However, the form (A.2) and (A.3) cannot accommodate the alternative proposal for the finite strain range wherein the total loading compliances are those from a nonlinear elastic solid. In general, there is no reason why $\mathbf{C}$ should be a linear combination of $\mathscr{M}'$ and $\boldsymbol{\omega} \otimes \boldsymbol{\omega}$, and thus the formulation based on (2.9) and (2.13) must be regarded as the fundamental one.

When the equivalence does hold, (A.2) and (A.3) have the advantage that they give rise to an explicit inversion of the rate law, as noted in conjunction with (3.15) for J_2 corner theory. For a general $\mathscr{M}$, CHRISTOFFERSEN (1978) has shown that

$$W(\boldsymbol{\varepsilon}) = \tfrac{1}{2}P(\alpha)\mathscr{L}'\boldsymbol{\varepsilon}\boldsymbol{\varepsilon} + \tfrac{1}{2}\mathscr{L}''\boldsymbol{\varepsilon}\boldsymbol{\varepsilon} \tag{A.4}$$

and

$$\cos\alpha = \frac{\mathscr{L}'\boldsymbol{\omega}\boldsymbol{\varepsilon}}{(\mathscr{L}'\boldsymbol{\omega}\boldsymbol{\omega})^{\frac{1}{2}}(\mathscr{L}'\boldsymbol{\varepsilon}\boldsymbol{\varepsilon})^{\frac{1}{2}}} \tag{A.5}$$

along with (3.14), (3.16) and the dual equations for convexity. Here, $\mathscr{L} = \mathscr{M}^{-1}$ and

$$\mathscr{L}' = \mathscr{L}\mathscr{M}'\mathscr{L} = \mathscr{L} - K\boldsymbol{\delta} \otimes \boldsymbol{\delta} \quad \text{and} \quad \mathscr{L}'' = \mathscr{L}\mathscr{M}''\mathscr{L} = K\boldsymbol{\delta} \otimes \boldsymbol{\delta}. \tag{A.6}$$

The orthogonality of the decomposed elastic moduli and compliances, i.e. $\mathscr{L}'\mathscr{M}'' = 0$ and $\mathscr{L}''\mathscr{M}' = 0$, are necessary prerequisites for the duality properties involving the stress-rate and the total strain-rate in this formulation.